it causes a 10-fold rate *decrease*; and in the reaction with $Co(o\text{-phen})_3^{3+}$, it causes a 2-fold rate *increase*.

In the reaction of $M^-$ with $Co(o\text{-phen})_3^{3+}$ as reported in this manuscript, the concentration of ions is large ($\sim 10^{-2}$ M). To ascertain a possible effect of ionic strength, we have examined this reaction and a few other reactions in the presence of excess $[NBu_4][BF_4]$ (0.01 → 0.04 M). For reaction of $[PPN][Re(CO)_5^-]$ with $[Co(o\text{-phen})_3][PF_6]$, addition of $[NBu_4][BF_4]$ led to a small decrease in rate, $k_{obs} = 1.8 \pm 0.1\ s^{-1}$ for $[[NBu_4][BF_4]] = 0$ M, $k_{obs} = 1.4 \pm 0.2$ for $[[NBu_4][BF_4]] = 0.020$ M. A similar small decrease in rate is observed when 3-acetoxy-*N*-methylpyridinium is reacted with $Re(CO)_5^-$ in the presence of $[NBu_4][BF_4]$. Reaction of $Ru_3(CO)_{12}$ with $Re(CO)_5^-$ is slowed by a factor of 4 in the presence of excess salt. For none of these reactions are ionic effects a dominant factor in the overall reaction rate.

**Conclusion.** In this manuscript we have examined the outer-sphere electron-transfer reactions of a series of metal carbonyl anions with $Co(o\text{-phen})_3^{3+}$ and with 3-acetoxy-*N*-methylpyridinium. There exists only a small change in reactivity with the nature of the metal carbonyl anion. Structures of $Mn(CO)_5^-$ and $Mn(CO)_4PEt_3^-$ show that the expected increase in potential by the $PEt_3$ donor is offset by an increased intrinsic barrier due to shortening of the Mn–CO bonds for the $PEt_3$ complex. The effect of the $Na^+$ counterion is small and unpredictable for the reactions of metal carbonyl anions. The presence of a noninteracting salt causes a small decrease in the rate of reaction of $Re(CO)_5^-$ with $Co(o\text{-phen})_3^{3+}$ or with 3-acetoxy-*N*-methylpyridinium. The very small effect of the nature of the metal carbonyl anion is the most diagnostic feature for an outer-sphere reaction.

**Acknowledgment.** We acknowledge the Department of Energy (Grant ER 13775) for support of this research, and we thank William Feighery and Jerry Keister for helpful discussions.

**Registry No.** $[PPN^+][Mn(CO)_5^-]$, 137203-43-1; $[PPN^+][Mn(CO)_4(PEt_3)^-]\cdot THF$, 137428-92-3; $[PPN^+][CpFe(CO)_2^-]$, 122521-41-9; $[PPN^+][CpRe(CO)_5^-]$, 119207-87-3; $[PPN^+][CpMo(CO)_3^-]$, 67486-18-4; $[Co(o\text{-phen})_3][PF_6]_3$, 28277-59-0; $[Co(o\text{-phen})_3][ClO_4]_3$, 14516-66-6; $Fe(o\text{-phen})_3^{3+}$, 13479-49-7; $CpFe(CO)_2^-$, 12107-09-4; $Re(CO)_5^-$, 14971-38-1; $Mn(CO)_5^-$, 35816-56-9; $CpMo(CO)_3^-$, 12126-18-0; $Mn(CO)_4PEt_3^-$, 137328-86-0; $Mn(CO)_4PBu_3^-$, 122521-42-0; $Mn(CO)_4PPh_3^-$, 53418-18-1; $[PPN][Co(CO)_4]$, 53433-12-8; $[Na][Re(CO)_5]$, 33634-75-2; $Re_2(CO)_{10}$, 14285-68-8; $Mn_2(CO)_{10}$, 10170-69-1; $Co_2(CO)_8$, 10210-68-1; $Cp_2Fe_2(CO)_4$, 12154-95-9; $Cp_2Mo_2(CO)_6$, 12091-64-4; 3-acetoxy-*N*-methylpyridinium tetrafluoroborate, 121758-03-0.

**Supplementary Material Available:** For $[PPN^+][Mn(CO)_5^-]$, tables of microanalyses, infrared spectral data, sample rate constant data, anisotropic thermal parameters, and H atom positions and sample absorbance plots and, for $[PPN][Mn(CO)_4(PEt_3)]\cdot THF$, tables of anisotropic thermal parameters and H atom positions (14 pages); listings of observed and calculated structure factors for $[PPN^+][Mn(CO)_5^-]$ and $[PPN][Mn(CO)_4(PEt_3)]\cdot THF$ (37 pages). Ordering information is given on any current masthead page.

# Kinetics and Mechanisms of CO Substitution of $(\eta^5\text{-Ind})Re(CO)_3$ (Ind = Indenyl) with Phosphines and Phosphites. The Indenyl Ligand Effect on Related Trindenylmetal Carbonyls

Hyochoon Bang,[†] Thomas J. Lynch,*[,‡,§] and Fred Basolo*[,†]

*Departments of Chemistry, Northwestern University, Evanston, Illinois 60208-3113, and University of Nevada, Reno, Nevada 89557-0020*

*Received May 14, 1991*

Kinetic studies were performed for the reactions of $(\eta^5\text{-Ind})Re(CO)_3$ with phosphines and phosphites. Second-order rate laws were observed, which are first-order in metal complex and first-order in phosphine concentrations. Depending on reaction conditions, i.e., temperature and ligand concentration, two different types of products, $(\eta^1\text{-Ind})Re(CO)_3L_2$ and $(\eta^5\text{-Ind})Re(CO)_2L$, were observed. The $\eta^1$-product changed slowly to $\eta^5$-product at high temperature. A reaction mechanism which requires a common intermediate for the formation of $\eta^1$- and $\eta^5$-products is proposed, which allows for simulated spectral changes in accord with what is observed experimentally. Also the reactivity of related trindenyl analogues were compared with indenyl- and cyclopentadienylmetal carbonyl complexes. The rates of reaction follow the order $(\eta^5\text{-Ind})M(CO)_n > (\eta^5\text{-Td})[M(CO)_n]_3 > (\eta^5\text{-Cp})Mo(CO)_n$, where M = Rh ($n = 2$) and Re and Mn ($n = 3$). For a given cyclic ligand, the rates decrease in the order Rh > Re > Mn; for changes in the number of $Re(CO)_3$ groups on a trindenyl ligand, the rates decrease in the order $(\eta^5\text{-TdH}_2)Re(CO)_3 > (\eta^5\text{-TdH})[Re(CO)_3]_2 > (\eta^5\text{-Td})[Re(CO)_3]_3$. These relative rates of reaction are discussed in terms of the coordination number of the metal, its size, and the extent of $\pi$-delocalization of electron density in the transition state for reaction.

## Introduction

We reported[1] in 1966 our observations that certain 18-electron organometallic compounds readily undergo associative ligand substitution, providing it is possible to localize a pair of electrons on one of the ligands in order to permit reaction via an 18-electron transition state/active intermediate. Reported in the same year was the ligand NO,[1a] which does this by the formation of $sp^2$ bent nitrosyl, and cyclopentadienyl[1b] and arene[1c] ligands, which involve "ring-slippage" mechanisms.[2] Many examples of this $\eta^5$

[†] Northwestern University.
[‡] University of Nevada.
[§] Present address: Hoechst-Celenese, 500 Washington St., Coventry, RI 02816.

(1) (a) Thorsteinson, E. M.; Basolo, F. *J. Am. Chem. Soc.* **1966**, *88*, 3929. (b) Schuster-Woldan, H. G.; Basolo, F. *J. Am. Chem. Soc.* **1966**, *88*, 1657. (c) Zingales, F.; Chiesa, A.; Basolo, F. *J. Am. Chem. Soc.* **1966**, *88*, 2707.

0276-7333/92/2311-0040$03.00/0 

→ $\eta^3$ → $\eta^5$ mechanism have been reported[2] for cyclopentadienyl compounds (eq 1). A similar mechanism[3a]

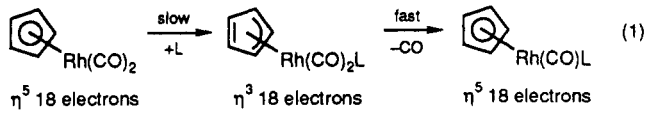


$\eta^5$ 18 electrons $\eta^3$ 18 electrons $\eta^5$ 18 electrons (1)

is believed to be responsible for the *indenyl ligand effect*,[3b] where the driving force for the more rapid $\eta^5$-indenyl versus $\eta^5$-cyclopentadienyl ligand substitution is believed to be the achievement of full aromaticity of the benzene ring in the transition state for reaction (eq 2). Structures have been determined by single-crystal X-ray crystallography of stable $\eta^3$-Cp[4a] and $\eta^3$-Ind[4b] metal complexes.

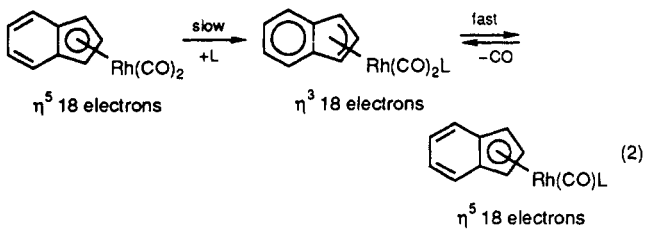


$\eta^5$ 18 electrons $\eta^3$ 18 electrons $\eta^5$ 18 electrons (2)

Casey[5a] and Werner[5b] independently reported the first examples of ring-slippage conversion of an $\eta^5$-Cp to an isolable $\eta^1$-Cp metal complex. Each proposed that the conversion involved in $\eta^5$ → $\eta^3$ → $\eta^1$ mechanism. Furthermore, Casey and O'Connor[6] report an attempt to obtain direct definitive evidence for the formation of ($\eta^3$-Ind)Re(CO)$_3$L as an active intermediate in the conversion of ($\eta^5$-Ind)Re(CO)$_3$ to ($\eta^1$-Ind)Re(CO)$_3$L$_2$. This was a perfectly plausible thing to try, because $\eta^3$-Ind systems are known to be more stable than are $\eta^3$-Cp systems. They followed the rapid reaction of ($\eta^5$-Ind)Re(CO)$_3$ with P(CH$_3$)$_3$ in $CD_2Cl_2$ at −65 °C with $^1$H NMR spectroscopy and obtained no evidence for an ($\eta^3$-Ind)Re(CO)$_3$L intermediate, even though estimates suggest that 5–10% of it would have been easily detected.

This present paper reports additional kinetic studies on the reaction of ($\eta^5$-Ind)Re(CO)$_3$ with P(OC$_2$H$_5$)$_3$ under four different conditions which selectively give predominately ($\eta^1$-Ind)Re(CO)$_3$[P(OEt)$_3$]$_2$, ($\eta^5$-Ind)Re(CO)$_2$P(OEt)$_3$, or a mixture of both. The results obtained under each of the four conditions are interpreted as involving a common intermediate, presumably ($\eta^3$-Ind)Re(CO)$_3$P(OEt)$_3$. Also reported are comparisons of rates of reaction of $\eta^5$-indenyl metal complexes with corresponding $\eta^5$-trindenyl[7] (see structure I) compounds.

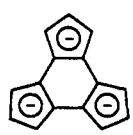

I (Td$^{3-}$)

(2) O'Connor, J. M.; Casey, C. P. *Chem. Rev.* **1987**, *87*, 307.
(3) (a) Hart-Davis, A. J.; Mawby, R. J. *J. Chem. Soc. A* **1969**, 2403. Jones, D. J.; Mawby, R. J. *Inorg. Chim. Acta* **1972**, *6*, 157. (b) Ji, L. N.; Rerek, M. E.; Basolo, F. *Organometallics* **1984**, *3*, 740.
(4) (a) Huttner, G.; Brintzinger, H. H.; Bell, L. G.; Friedrich, P.; Bejenke, V.; Neugebrauer, D. *J. Organomet. Chem.* **1978**, *145*, 329. (b) Nesmeyanov, A. N.; Ustynyuk, N. A.; Makarova, L. G.; Andrianov, V. G.; Struchkov, Y. T.; Andrae, S.; Ustynyuk, Y. A.; Malyugina, S. G. *J. Organomet. Chem.* **1979**, *159*, 189. Kowaleski, R. M.; Rheingold, A. L.; Trogler, W. C.; Basolo, F. *J. Am. Chem. Soc.* **1986**, *108*, 2460.
(5) (a) Casey, C. P.; Jones, W. D. *J. Am. Chem. Soc.* **1980**, *102*, 6154. (b) Werner, H.; Kuhn, A.; Burschka, C. *Chem. Ber.* **1980**, *113*, 2291.
(6) Casey, C. P.; O'Conner, J. M. *Organometallics* **1985**, *4*, 384.
(7) (a) Lynch, T. J.; Helventon, M. C.; Rheingold, A. L.; Staley, D. L. *Organometallics* **1989**, *8*, 1959. (b) Helventon, M. C.; Lynch, T. J. *J. Organomet. Chem.* **1989**, *359*, C50. (c) Katz, T. J.; Slusarek, W. *J. Am. Chem. Soc.* **1980**, *102*, 1058.

**Table I. Carbonyl Stretching Frequencies for Metal Complexes in Decalin**

| complexes | $\nu_{CO}$, cm$^{-1}$ |
|---|---|
| ($\eta^5$-Ind)Re(CO)$_3$ | 2027 (s), 1939 (s), 1932 (s) |
| ($\eta^1$-Ind)Re(CO)$_3$[P(n-Bu)$_3$]$_2$ | 2009 (m, br), 1925 (m, br), 1885 (m, br)[a] |
| ($\eta^1$-Ind)Re(CO)$_3$[P(OEt)$_3$]$_2$ | 2034 (m, br), 1958 (m, br), 1908 (m, br) |
| ($\eta^1$-Ind)Re(CO)$_3$[P(OPh)$_3$]$_2$ | 2059 (m, br), 1995 (m, br), 1931 (m, br) |
| ($\eta^1$-Ind)Re(CO)$_3$(diphos)$_2$ | 2014 (m, br), 1939 (m, br), 1905 (m, br)[a] |
| ($\eta^1$-Ind)Re(CO)$_3$[PCy$_3$]$_2$ | 2008 (m, br), 1930 (m, br), 1883 (m, br) |
| ($\eta^5$-Ind)Re(CO)$_2$[P(OEt)$_3$] | 1951 (s, br), 1885 (s, br) |
| ($\eta^5$-Ind)Re(CO)$_2$[P(OPh)$_3$] | 1967 (s, br), 1902 (s, br) |
| ($\eta^5$-Ind)Re(CO)$_2$[PCy$_3$] | 1929 (s, br), 1862 (s, br) |
| ($\eta^5$-TdH$_2$)Re(CO)$_3$ | 2020 (s), 1927 (s, br)[a] |
| ($\eta^1$-TdH$_2$)Re(CO)$_3$[P(OEt)$_3$]$_2$ | 2035 (m, br), 1970 (m, br), 1905 (m, br)[a] |
| ($\eta^5$-TdH$_2$)Re(CO)$_2$[P(OEt)$_3$] | 1945 (s, br), 1870 (s, br)[a] |
| ($\eta^5$-Td)[Re(CO)$_3$]$_3$ | 2038 (m), 2025 (s), 1952 (s, br), 1934 (s, br)[a] |
| ($\eta^1$-Td)[Re(CO)$_3$[P(n-Bu)$_3$]$_2$]$_3$ | 2016 (m), 1927 (m, br), 1895 (m, br)[a] |
| ($\eta^5$-Td)[Re(CO)$_2$P(n-Bu)$_3$]$_3$ | 2026 9w), 2007 (w), 1923 (s, br), 1889 (w, br)[a] |
| ($\eta^5$-Td)[Mn(CO)$_3$]$_3$ | 2032 (m), 2020 (s), 1956 (s, br), 1938 (s, br)[b] |
| ($\eta^5$-Td)[Rh(CO)$_2$]$_3$ | 2035 (s), 1975 (s) |
| ($\eta^5$-Td)[Rh(CO)PPh$_3$]$_3$ | 1956 (s) |
| ($\eta^5$-Td)[Rh(CO)P(n-Bu)$_3$]$_3$ | 1943 (s) |

[a] Solvent was toluene. [b] Solvent was THF.

## Experimental Section

**General Procedure.** All experimental operations were carried out under an atmosphere of $N_2$ by using standard Schlenk techniques. Decalin, toluene, hexane, and THF were distilled over Na under a $N_2$ atmosphere. Decalin and toluene used for kinetics were bubbled with $N_2$ for 1 h after distillation. The phosphines used in these studies were obtained from Strem of Aldrich Chemicals. All phosphines were distilled from Na using a $N_2$ atmosphere prior to use.

**Compounds.** The metal complexes used in this study were prepared by standard literature procedures and characterized by comparison of their IR spectra with the known spectra of the compounds.[7,8] The IR spectra of the substrates used and of the products obtained are given in Table I. Not previously reported are the compounds ($\eta^5$-Td)[Rh(COD)]$_3$ (COD = cyclooctadiene) and ($\eta^5$-Td)[Rh(CO)$_2$]$_3$.

**The synthesis of ($\eta^5$-Td)[Rh(COD)]$_3$** is similar to the methods used to prepare other trindenyl complexes reported earlier:[7] A 10-mL Schlenk flask charged with dihydro-1*H*-trindene[7] (22 mg, 0.11 mmol) and 4 mL of dry THF was cooled to −78 °C, and *n*-BuLi in hexanes (0.15 mL, 0.36 mmol) was added with stirring. After 15 min the cold bath was removed and stirring continued for 1 h to give a colorless solution and a white precipitate. The mixture was again cooled to −78 °C, and [Rh(COD)Cl]$_2$ (Strem, 88 mg, 0.18 mmol) was added under a blanket of nitrogen. The cold bath was replaced with a room-temperature water bath. Within 5 min all solids dissolved, and in 15 min a yellow solid began to form. Stirring was continued for 8 h. The supernatant was decanted, and the yellow solid was placed under vacuum for 2 h. Extraction into 25 mL of benzene followed by filtration and vacuum removal of solvent from the filtrate yielded 82 mg of ($\eta^5$-Td)[Rh(COD)]$_3$ (91% based on dihydro-1*H*-trindene). $^1$H and $^{13}$C NMR spectra parallel those of other trindenyl compounds:[7] $^1$H NMR ($C_6D_6$) $\delta$ 5.36 (td, 1, $J$ = 2.8, 1.1 Hz), 5.31 (td, 2, $J$ = 2.6, 1.0 Hz), 5.11 (dd, 2, $J$ = 2.5, 1.4 Hz), 4.98 (dd, 2, $J$ = 2.5, 1.4 Hz), 4.95 (d, 2, $J$ = 2.7 Hz), 4.03 (m, 4), 3.89 (m, 4), 3.67

(8) Casey, C. P.; O'Conner, J. M.; Jones, W. D.; Haller, K. *Organometallics* **1983**, *2*, 535.

**Scheme I**

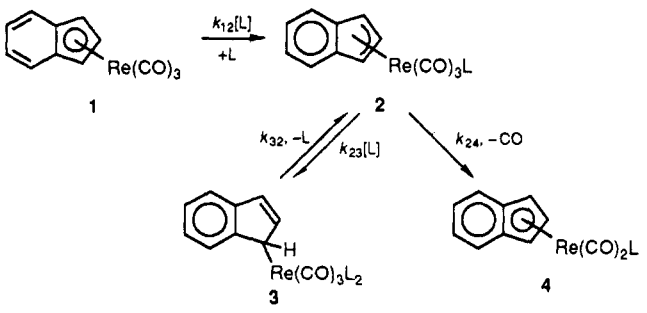


(m, 4), 1.7–2.4 (m, 24); $^{13}C\{^1H\}$ NMR ($C_6D_6$) δ 103.9 (d, $J$ = 3.1 Hz), 99.9 (d, $J$ = 3.4 Hz), 99.8 (d, $J$ = 3.3 Hz), 86.5 (d, $J$ = 4.3 Hz), 85.6 (d, 4.5 Hz), 79.8 (d, $J$ = 3.5 Hz), 78.8 (d, $J$ = 3.8 Hz), 77.3 (d, $J$ = 4.1 Hz), 68.23 (d, $J$ = 14.0 Hz), 68.19 (d, $J$ = 140 Hz), 67.2 (d, $J$ = 14.3 Hz), 34.1 (s), 32.5 (s), 31.9 (s).

**The synthesis of ($\eta^5$-Td)[Rh(CO)$_2$]$_3$** was then readily carried out by bubbling the CO gas through the solution of ($\eta^5$-Td)[Rh(COD)]$_3$ (35 mg) in 5 mL of toluene for 15 min at room temperature. An orange powder was obtained and purified by recrystallization from pentane. Its IR spectrum in the CO region is given in Table I.

**Instrumentation.** Infrared spectra were recorded on a Nicolet 5PC FT-IR spectrometer using a 0.2-mm KBr cells. For kinetic measurements the absorbance mode was used. Samples were thermostated with a silicon oil bath, and the temperature was regulated by a Cole-Parmer Digi-Sense temperature controller with a type J thermocouple. The uncertainty in the temperature of the reaction is placed at ±0.2 °C.

**Kinetic Measurement.** Decalin reaction mixtures of 5.0 mL were placed in the constant-temperature bath; 0.3-mL aliquots were removed periodically over 2–3 half-lives to measure the absorbance changes in the carbonyl stretching region. The IR cells were flushed with $N_2$ and sealed with rubber septa prior to use. The rates of reaction were monitored by measuring the decrease in the highest carbonyl absorption. Plots of ln $A$ vs time or ln ($A_\infty$–$A$) vs time were linear over 2–3 half-lives, and $k_{obsd}$ was determined from the slope of this line by the least-squares method. The correlation coefficient of the least-squares line ($R^2 > 0.995$) was very good. The error limits reported for values of $\Delta H^\ddagger$ and of $\Delta S^\ddagger$ were calculated from the standard errors of the slopes and intercepts obtained by the least-squares method. As usual, the confidence limits will differ depending on the number of experimental data points used. Approximately $1 \times 10^{-3}$ M solutions of metal complex were used, and all kinetic experiments were carried out under pseudo-first-order conditions with at least a 10-fold excess of nucleophile.

## Results

**Kinetics of ($\eta^5$-Ind)Re(CO)$_3$.** The reaction of excess P(OEt)$_3$ with ($\eta^5$-Ind)Re(CO)$_3$ (1) produced two different products depending on reaction conditions. At low temperature and high ligand concentration, ($\eta^1$-Ind)Re(CO)$_3$[P(OEt)$_3$]$_2$ (3) was the reaction product. But at high temperature and low ligand concentration, the product was ($\eta^5$-Ind)Re(CO)$_2$P(OEt)$_3$ (4). When the reaction conditions of temperature and ligand concentration were between these two extreme cases, both of the reaction products appeared simultaneously. Part a–d of Figure 1 clearly show these changing patterns. For example, in the case of Figure 1c the $\eta^1$-species (3) grew fast initially and then decreased and disappeared completely, and the final product became $\eta^5$-species (4). The experimental observations, shown in Figure 1a–d, are interpreted in the Discussion in terms of the reactions in Scheme I. This reaction scheme is the same as that proposed by Casey[8] for the reaction of ($\eta^5$-Cp)Re(CO)$_3$ with PMe$_3$, whereas no mention was made earlier[6] of the formation of ($\eta^5$-Ind)Re(CO)$_2$L.

**Table II. Pseudo-First-Order Rate Constants $10^3 k_{obsd}$ ($s^{-1}$) for the Reactions of ($\eta^5$-Ind)Re(CO)$_3$ with P(OEt)$_3$ in Decalin**

| [L][a] | 100 °C | 90 °C | 70 °C | 56 °C |
|---|---|---|---|---|
| 0.820 | | 6.02 | | 2.30 |
| 0.0700 | 6.40 | 5.49 | | 1.89 |
| 0.0583 | 5.29 | 3.52 | 2.30 | 1.62 |
| 0.0466 | 4.02 | 3.19 | | |
| 0.0400 | | | 1.55 | |
| 0.0350 | 3.00 | | | |
| 0.0233 | 1.88 | | 0.71 | 0.44 |
| 0.0175 | | | | 0.28 |
| 0.0117 | 0.72 | | 0.28 | 0.15 |

[a] Concentration of P(OEt)$_3$ in the unit of mol/liter.

**Table III. Second-Order Rate Constant[a] and Activation Parameters[b] for the Reactions of ($\eta^5$-Ind)Re(CO)$_3$ with P(OEt)$_3$ in Decalin**

| $T$, °C | $10^2 k_{12}$, $M^{-1}$ $s^{-1}$ | $10^4 k_{32}$, $s^{-1}$ [b] | $k_{23}/k_{24}$ [d] |
|---|---|---|---|
| 100 | 10.5 | 7.67 | 40 |
| 90 | 8.87 | 2.48 | 49 |
| 80 | | 0.701 | |
| 70 | 4.41 | 0.227 | 157 |
| 56 | 3.10 | | 324 |

[a] Rate constants $k_{12}$, $k_{23}$, $k_{24}$, and $k_{32}$ are defined in Scheme II. [b] $\Delta H_{12}^\ddagger$ = 6.4 (±0.5) kcal/mol, $\Delta H_{32}^\ddagger$ = 29.3 (±0.8) kcal/mol, $\Delta S_{12}^\ddagger$ = -46 (±2) eu, $\Delta S_{32}^\ddagger$ = 5 (±2) eu, $\Delta H_{23}^\ddagger - \Delta H_{24}^\ddagger$ = 12.9 (±0.9) kcal/mol, and $\Delta S_{23}^\ddagger - \Delta S_{24}^\ddagger$ = -39 (±3) eu. [c] From eq 2, the expected $k_{32}$ at 100 °C = $1.81 \times 10^{-3}$ $s^{-1}$ and $k_{32}$ at 90 °C = $5.29 \times 10^{-4}$ $s^{-1}$. [d] No unit. Also see eqs 2 and 3.

**Table IV. Second-Order Rate Constants and Activation Parameters for the Reactions of ($\eta^5$-Ind)Re(CO)$_3$ + L**

| L[a] | $T$, °C | $k_{12}$, $M^{-1}$ $s^{-1}$ | activation params[b] |
|---|---|---|---|
| P($n$-Bu)$_3$ | 10 | $1.2 \times 10^{-2}$ | $\Delta H_{12}^\ddagger$ = 8.4 (±1.0) |
| | 0 | $5.8 \times 10^{-3}$ | $\Delta S_{12}^\ddagger$ = -37 (±4) |
| | -10 | $3.5 \times 10^{-3}$ | |
| P(OPh)$_3$ | 90 | $1.0 \times 10^{-3}$ | $\Delta H_{12}^\ddagger$ = 15.0 (±1.1) |
| | 100 | $1.7 \times 10^{-3}$ | $\Delta S_{12}^\ddagger$ = -31 (±3) |
| | 110 | $3.1 \times 10^{-3}$ | |

[a] The solvent was toluene for P($n$-Bu)$_3$ and decalin for P(OPh)$_3$. [b] The unit of $\Delta H_{12}^\ddagger$ is kcal/mol, and the unit of $\Delta S_{12}^\ddagger$ is eu.

Under pseudo-first-order reaction conditions, the rate of disappearance of ($\eta^5$-Ind)Re(CO)$_3$ is first-order in substrate and in P(OEt)$_3$ concentration (Table II). A plot of $k_{obsd}$ vs [P(OEt)$_3$] (Figure 2) shows this is a second-order reaction, and within experimental error the points clearly extrapolate through the origin indicating no contribution from a first-order parallel pathway. Second-order rate constants and activation parameters for the reaction are given in Table III.

In order to further test the validity of Scheme I, ($\eta^1$-Ind)Re(CO)$_3$[P(OEt)$_3$]$_2$ was isolated and its rate of conversion to ($\eta^5$-Ind)Re(CO)$_2$P(OEt)$_3$ was determined. It was also observed that this rate is unaffected by the presence of CO (1 atm).

Reactions of ($\eta^5$-Ind)Re(CO)$_3$ (first step in Scheme I) were investigated with ligands other than P(OEt)$_3$. For P($n$-Bu)$_3$ and P(OPh)$_3$ the reactions are second-order, and the rate constants at different temperatures along with activation parameters are given in Table IV. For PMePh$_2$ and PMe$_2$Ph, PCy$_3$, and diphos runs at only one concentration were made, with the results of $k_{obsd}$ = $1.30 \times 10^{-3}$ $s^{-1}$ ([PMePh$_2$] = 0.07 M, $T$ = 0 °C), $k_{obsd}$ = $1.62 \times 10^{-4}$ $s^{-1}$ ([PMe$_2$Ph] = 0.53 M, $T$ = 0 °C), $k_{obsd}$ = $5.05 \times 10^{-6}$ $s^{-1}$ ([PCy$_3$] = 0.01 M, $T$ = 100 °C), and $k_{obsd}$ = $4.01 \times 10^{-1}$ ([diphos] = 0.06 M, $T$ = 70 °C). Values of $\Delta G_{12}^\ddagger$, along with cone angles and basicities, of all entering ligands studied are given in Table V.

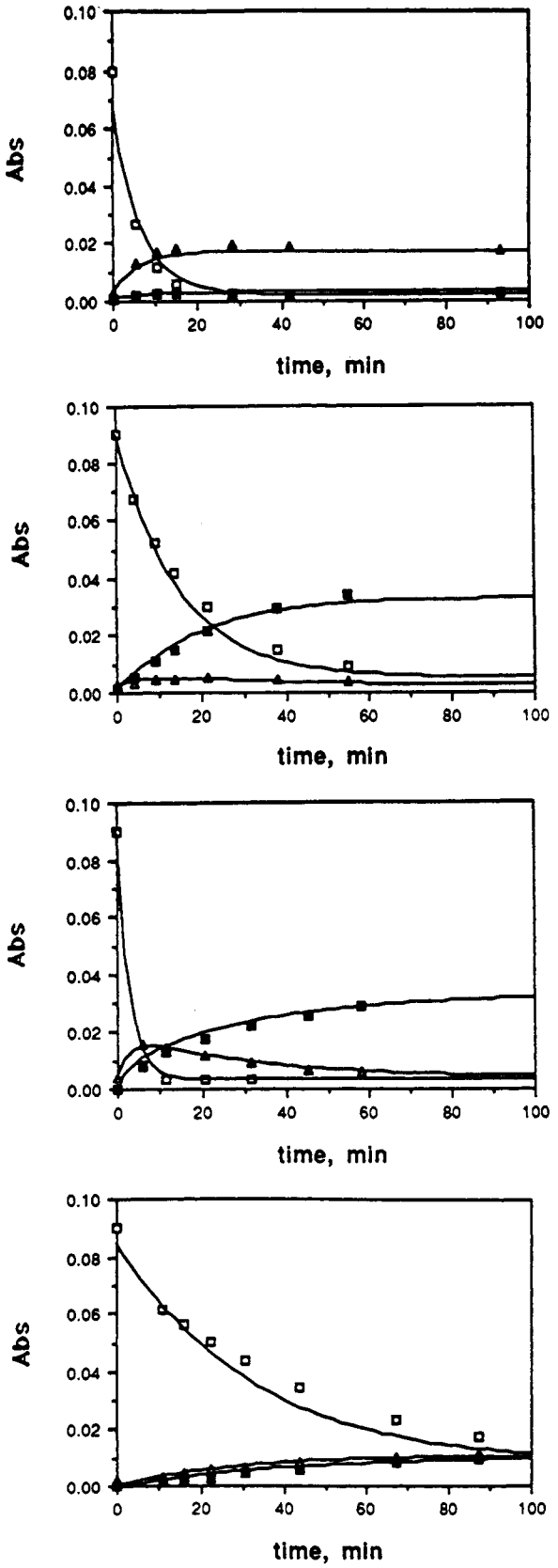


**Figure 1.** Absorption changes of each species for the reactions of IndRe(CO)$_3$ with P(OEt)$_3$ in decalin. Experimental data points are shown by each symbol, and the curves on the plot are simulated curves of eqs 21–23 (see text). The symbols are □ = ($\eta^5$-Ind)Re(CO)$_3$, ▲ = ($\eta^1$-Ind)Re(CO)$_3$L$_2$, and ■ = ($\eta^5$-Ind)Re(CO)$_2$L, where L = P(OEt)$_3$. Key (from top to bottom): (a) low $T$ and high [L] ($T$ = 70 °C, [] = 0.058 M); (b) high $T$ and low [L] ($T$ = 100 °C, [L] = 0.012 M); (c) high $T$ and high [L] ($T$ = 100 °C, [L] = 0.058 M); (d) low $T$ and low [L] ($T$ = 70 °C, [L] = 0.012 M).

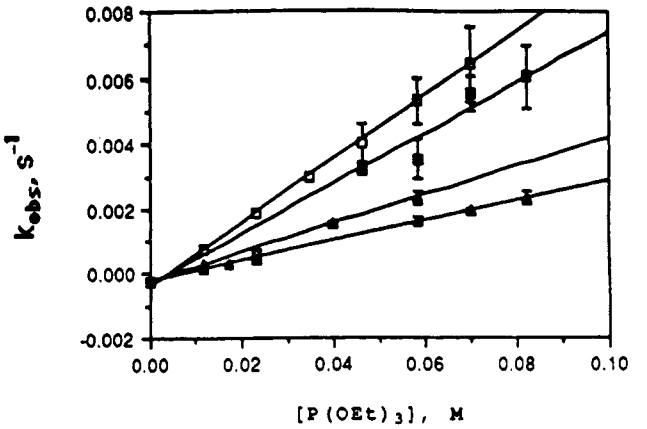


**Figure 2.** Plot of $k_{obsd}$ vs [P(OEt)$_3$] concentration for the reaction of IndRe(CO)$_3$ with P(OEt)$_3$ in decalin: □ = 100 °C; ■ = 90 °C; △ = 70 °C; ▲ = 56 °C. The uncertainty of each data point is indicated by small $y$ bar.

**Table V. Free Energies of Activation, $\Delta G^*$, for the Reactions of ($\eta^5$-Ind)Re(CO)$_3$ + L**

| L | solvent | $T$, °C | $\Delta G_{12}{}^{*a}$ | $\theta^b$ | p$K_a$ |
|---|---|---|---|---|---|
| $PCy_3$ | decalin | 100 | 28 | 170 | 9.70 |
| $P(OPh)_3$ | decalin | 100 | 27 | 128 | -2.00 |
| $P(OEt)_3$ | decalin | 100 | 23 | 109 (137)$^c$ | 3.31 |
| $PMePh_2$ | toluene | 0 | 20 | 136 | 4.57 |
| diphos$^d$ | toluene | 70 | 19 | | |
| P($n$-Bu)$_3$ | toluene | 0 | 19 | 132 | 8.43 |
| $PMe_2Ph$ | toluene | 0 | 18 | 122 | 6.50 |
| $PMe_3$$^e$ | $CD_2Cl_2$ | -65 | 15 | 118 | 8.65 |

$^a$ The unit is kcal/mol. $\Delta G_{12}{}^* = 1.987T(23.76 + \ln T - \ln k_{12})$. $^b$ Reference 10; ligand cone angle in degrees. $^c$ Revised cone angle in: Lothar, S.; Ernst, R. D. *J. Am. Chem. Soc.* **1987**, *109*, 5673. $^d$ diphos = $Ph_2PCH_2CH_2PPh_2$; $\theta$ and p$K_a$ values are expected to be similar to those of $PMePh_2$. $^e$ Reference 6.

**Kinetics of Trindenylrhenium Complexes.** The reaction of ($\eta^5$-TdH$_2$)Re(CO)$_3$ (see structure II) with P(OEt)$_3$

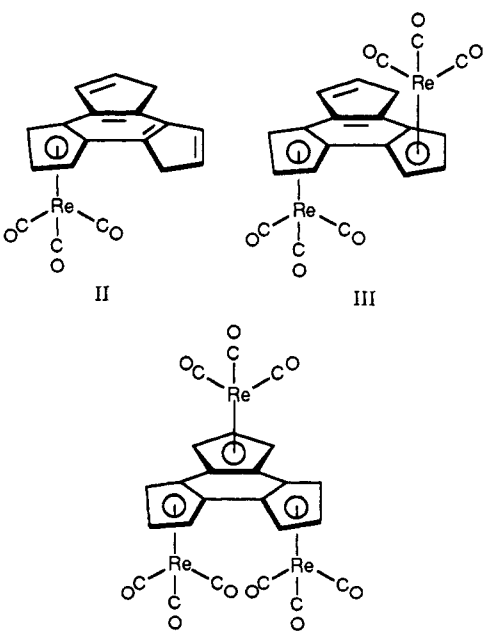


in toluene at 40 °C affords ($\eta^1$-TdH$_2$)Re(CO)$_3$[P(OEt)$_3$]$_2$ with $k_{obsd}$ = 9.6 × 10$^{-5}$ s$^{-1}$ ([P(OEt)$_3$] = 0.233 M) and 2.2 × 10$^{-4}$ s$^{-1}$ ([P(OEt)$_3$] = 0.47 M). When the reaction temperature was increased to 80 °C, the $\eta^1$-species CO bands in the IR spectrum decrease and new bands of the $\eta^5$-product appear. At higher temperatures, with [P(OEt)$_3$]

Table VI. Pseudo-First-Order Rate Constants and Activation Parameters for the Reaction of $Td[Rh(CO)_2]_3$ with $P(n\text{-}Bu)_3$ in Decalin

| T, °C | [L][a] | $k_{obsd}$, $s^{-1}$ | activation params |
|---|---|---|---|
| 0 | 0.08 | $3.2 \times 10^{-4}$ | $\Delta H_{12}^{\ddagger} = 8.9$ (±0.4) |
| | 0.32 | $1.3 \times 10^{-3}$ | |
| | 0.80 | $3.6 \times 10^{-3}$ | |
| 10 | 0.08 | $6.2 \times 10^{-4}$ | $\Delta S_{12}^{\ddagger} = -37$ (±2) |
| 19 | 0.08 | $1.0 \times 10^{-3}$ | |

[a] Concentration of $P(n\text{-}PBu)_3$.

= 0.082 M, $k_{obsd} = 8.07 \times 10^{-4}$ $s^{-1}$ at 70 °C and $k_{obsd} = 1.22 \times 101^{-3}$ $s^{-1}$ at 90 °C. A couple of kinetic runs were done with trindenyltris(rhenium tricarbonyl) (see structure IV), $(\eta^5\text{-Td})[Re(CO)_3]_3$, using $P(n\text{-}Bu)_3$ in toluene at 70 °C. The results obtained are $k_{obsd} = 7.63 \times 10^{-5}$ $s^{-1}$ at $[P(n\text{-}Bu)_3]$ = 0.401 M and $k_{obsd} = 3.34 \times 10^{-5}$ $s^{-1}$ at $[P(n\text{-}Bu)_3]$ = 0.200 M.

Reaction rates of $PMe_2Ph$ (0.06 M in THF) with trindenyl complexes at room temperature decrease in the order II > III > IV, where $t_{1/2}$ equal 7 min, 11 min, and no reaction, respectively.

Also studied was the rhodium compound $(\eta^5\text{-Td})[Rh(CO)_2]_3$. Its reaction with $P(n\text{-}Bu)_3$ affords $(\eta^5\text{-Td})[Rh(CO)P(n\text{-}Bu)_3]_3$, presumably by the $\eta^5 \rightarrow \eta^3 \rightarrow \eta^5$ process reported earlier[1b] for the reactions of $(\eta^5\text{-Cp})Rh(CO)_2$. Observed rate constants, $k_{obsd}$, and activation parameters for the reaction are given in Table VI. Second-order rate constants for reactions of $(\eta^5\text{-Td})[Rh(CO)_2]_3$ are compared with the rate constants known for similar reactions of $(\eta^5\text{-Cp})Rh(CO)_2$ and of $(\eta^5\text{-Ind})Rh(CO)_2$ (Table VII). Comparisons of values for the free energies of activation for several analogues systems are tabulated (Table VIII).

## Discussion

**Reactions of $(\eta^5\text{-Ind})Re(CO)_3$ with $P(OEt)_3$.** These reactions are believed to proceed by Scheme I, and by applying the steady-state approximation for the active intermediate **2**, it is possible to estimate rate constants $k_{12}$, $k_{32}$, and the ratio $k_{23}/k_{24}$ (Scheme I). This treatment of the kinetic data establishes that the $\eta^1$-**3** and the $\eta^5$-**4** products derive from a common transition-state/active-intermediate **2**; however, it does not establish the nature of this common intermediate **2**. Its assignment as the $\eta^3$-species is consistent with all prior studies on such systems[2] and with the concept of maintaining an 18-electron count[1] throughout the reaction pathways.

Rate constants $k_{12}$ can be directly determined for any entering ligand by following the rate of disappearance of substrate **1**. Rate constant $k_{32}$ can be directly determined by starting with an isolated sample of the $\eta^1$-compound (**3**) and monitoring its rate of disappearance. The ratio of rate constants $k_{23}/k_{24}$ is evaluated from a steady-state treatment of the kinetic data. Using these rate constants and the molar absorbances of **1**, **3**, and **4**, it is a possible to simulate the absorbance change of a given reaction mixture. This was done (Figure 1a–d, where the points are experimental and the lines are estimated) with satisfactory results for four different experimental conditions, as per the following discussion.

**Reaction Conditions. (a) Low Temperature and High Ligand Concentration.** These experimental conditions are met when $T$ = 70 or 56 °C and $[P(OEt)_3] > 0.04$ M. Under these conditions, spectral changes (Figure 1a) show the main product is $\eta^1$-**3** with a negligible amount of $\eta^5$-**4**. This means the reaction mechanism of Scheme I can be simplified (eq 3). Thus, the steady-state approximation

$$1 \xrightarrow{k_{12}[L]} 2 \xrightarrow{k_{23}[L]} 3 \qquad (3)$$

Table VII. Comparison of Second-Order Rate Constants and $\Delta G_{12}^{\ddagger}$ Values for the Reactions of $LRh(CO)_2$ with $PR_3$ in Toluene[a]

| L | $PR_3$[b] | T, °C | $k_{12}$, $M^{-1}$ $s^{-1}$ | $\Delta G_{12}^{\ddagger}$, kcal/mol |
|---|---|---|---|---|
| $\eta^5$-Cp[c] | $P(n\text{-}Bu)_3$ | 40 | $4.3 \times 10^{-3}$ | 22 |
| | $PPh_3$ | | $2.9 \times 10^{-4}$ | 23 |
| | $P(OPh)_3$ | | $7.3 \times 10^{-5}$ | 24 |
| $\eta^5$-Ind[d] | $PPh_3$ | 21 | $2.8 \times 10^{4}$ | 11 |
| $\eta^5$-Td[e] | $P(n\text{-}Bu)_3$ | 19 | $1.2 \times 10^{-2}$ | 20 |
| | $PPh_3$ | | $9.9 \times 10^{-3}$ | 20 |

[a] Decalin was used for the trindenyl system. [b] See Table V for cone angle and $pK_a$ values. [c] Reference 1b. [d] Reference 3b. [e] This work. The formula is $Td[Rh(CO)_2]_3$.

Table VIII. Free Energies of Activation, $\Delta G_{12}^{\ddagger}$, for the Reaction of $LM(CO)_x$[a] + $PR_3$

| M | L | $PR_3$ | T, °C | $\Delta G_{12}^{\ddagger}$[b] | ref |
|---|---|---|---|---|---|
| Mn | Cp | $PPh_3$ | 40 | no reacn | 1b |
| | Td[c] | $P(n\text{-}Bu)_3$ | 200 | no reacn | this work |
| | Ind | $P(OEt)_3$ | 130 | 32 | 3b |
| Re | Cp | $PMe_3$ | 88 | 29 | 6 |
| | Td[c] | $P(n\text{-}Bu)_3$ | 70 | 26 | this work |
| | Ind | $P(OEt)_3$ | 90 | 22 | this work |
| | | $PMe_3$ | −65 | 15 | 6 |
| Rh | Cp | $PPh_3$ | 40 | 23 | 1b |
| | Td[c] | $P(n\text{-}Bu)_3$ | 19 | 20 | this work |
| | Ind | $PPh_3$ | 21 | 11 | 3b |

[a] $x$ = 3 for Mn and Re; $x$ = 2 for Rh. [b] The unit is kcal/mol. [c] The formula is $(\eta^5\text{-Td})[M(CO)_x]_3$; $x$ = 3 for Mn and Re and $x$ = 2 for Rh.

for the intermediate $\eta^3$-**2** can now be applied because $k_{23}[L] \gg k_{12}[L]$. Then the rate law becomes as shown in eq 4,

$$\frac{-d[A_1]}{dt} = \frac{d[A_3]}{dt} = k_{obsd}[A_1] \qquad (4)$$

where $[A_1]$ and $[A_3]$ are concentrations of species **1** and **3**, respectively, and where $k_{obsd} = k_{12}[L]$. The rate of increase of **3** should be equal to the rate of decrease of **1**, which were monitored separately by following the change in absorbency at 1908 and 1939 $cm^{-1}$, respectively. For the reaction conditions of Figure 1a, the experimental results are in excellent agreement ($k_{obsd}$ for decreasing **1** = 2.30 (±0.20) × $10^{-3}$ $s^{-1}$; $k_{obsd}$ for increasing **3** = 2.48 (±0.09) × $10^{-3}$ $s^{-1}$). This kind of $\eta^5 \rightarrow \eta^3 \rightarrow \eta^1$ ring slippage was also reported by Casey[6,8] at relatively low temperatures in the case of $(\eta^6\text{-Cp})Re(CO)_3$ and of $(\eta^5\text{-Ind})Re(CO)_3$.

**(b) High Temperature and Low Ligand Concentration.** These conditions are met when $T$ = 100 or 90 °C and $[P(OEt)_3] < 0.025$ M. The spectral changes during reaction show (Figure 1b) that the product is $\eta^5$-**4**, with negligible amount of $\eta^1$-**3**. Therefore, the mechanism could be simplified (eq 5). At these conditions the steady-state

$$1 \xrightarrow{k_{12}[L]} 2 \xrightarrow{k_{24}} 4 \qquad (5)$$

assumption for **2** is based on $k_{24} \gg k_{12}[L]$, and the rate law is given by eq 6. This means the rate of reaction of **1**

$$\frac{-d[A_1]}{dt} = \frac{d[A_4]}{dt} = k_{obsd}[A_1] \qquad (6)$$

equals the rate of formation of **4**. At the experimental conditions of Figure 1b, good agreement in support of this treatment was obtained ($k_{obsd}$ for decreasing **1** = 7.18 (±0.18) × $10^{-4}$ $s^{-1}$; $k_{obsd}$ for increasing **4** = 7.63 (±0.27) × $10^{-4}$ $s^{-1}$). These results suggest primarily a reaction pathway of the type $\eta^5 \rightarrow \eta^3 \rightarrow \eta^5$ ring slippage, similar to that reported earlier for $(\eta^5\text{-Cp})Rh(CO)_2$[1b] and $(\eta^5\text{-Ind})Rh(CO)_2$.[3b] It should be noted (Scheme I) that there are two possible ways for making **4**, the first is **1** → **2** → **4** and the second is **1** → **2** → **3** → **2** → **4**. However, the net result,

1 → 4, is same for both processes, and the rate-determining step remains 1 → 2. It appears that the primary pathway for the formation of 4 is 1 → 2 → 4, but since small amounts of 3 do form, this can provide a minor pathway for the formation of 4. A discussion of this pathway immediately follows.

**(c) High Temperature and High Ligand Concentration.** These conditions are met when $T$ = 100 or 90 °C and [P(OEt)$_3$] > 0.04 M. The concentration changes of this reaction mixture shows (Figure 1c) that initially both the $\eta^1$-3 and $\eta^5$-4 species form. After approximately 10 min, the amount of starting material (1) is negligible, and 3 starts to decrease while 4 keeps increasing. After the first 10 min when compound 1 has completely reacted, it follows that the increased amount of 4 is due to the decreased amount of 3, so the pathways involved are given by eq 7. The assumption that $k_{24} \gg k_{32}$ and $k_{23}[L] \gg k_{32}$

$$3 \underset{k_{23}[L]}{\overset{k_{32}}{\rightleftharpoons}} 2 \xrightarrow{k_{24}} 4 \qquad (7)$$

gives the simplified rate law (eq 8). For the reaction

$$\frac{-d[A_3]}{dt} = \frac{d[A_4]}{dt} = k_{obsd}[A_3] \qquad (8)$$

conditions of Figure 1c, after the first 10 min, the experimental results are in excellent agreement ($k_{obsd}$ for decreasing 3 = 5.44 (±0.33) × $10^{-4}$ $s^{-1}$; $k_{obsd}$ for increasing 4 = 5.80 (±0.23) × $10^{-4}$ $s^{-1}$). This kind of $\eta^1 \rightarrow \eta^3 \rightarrow \eta^5$ ring slippage was reported by Casey[8] in the case of ($\eta^1$-Cp)Re(CO)$_3$[PMe$_3$]$_2$, which is converted into ($\eta^5$-Cp)Re(CO)$_2$[PMe$_3$] at elevated temperatures (100 °C).

**(d) Low Temperature and Low Ligand Concentration.** These conditions are met when $T$ = 70 or 56 °C and [P(OEt)$_3$] < 0.025 M. The spectral changes during reaction show (Figure 1d) that both of the products, $\eta^1$-3 and $\eta^5$-4, apparently coexist from the beginning. The low temperature favors the pathway to 3, but the low ligand concentration favors the pathway to 4. Therefore, the mechanism at the initial stage of reaction (before significant return of 3 to 2) can be viewed as in eq 9. On the assumption

$$1 \xrightarrow{k_{12}[L]} 2 \begin{cases} \xrightarrow{k_{23}[L]} 3 \\ \xrightarrow{k_{24}} 4 \end{cases} \qquad (9)$$

that $k_{23}[L] \gg k_{12}$ and $k_{24} \gg k_{12}$, this then gives a simplified rate law (eq 10). This requires that the rate of decrease

$$\frac{-d[A_1]}{dt} = \frac{d[A_3]}{dt} + \frac{d[A_4]}{dt} \qquad (10)$$

of 1 be equal to the sum of the rate of increase of 3 and 4. For the reaction conditions in Figure 1d at the initial stage of reaction, the experimental results are in good agreement (rate for decreasing 1 = 2.73 (±0.18) × $10^{-7}$ M/s; rate for increasing 3 = 2.07 (±0.01) × $10^{-7}$ M/s; rate for increasing 4 = 1.20 (±0.01) × $10^{-7}$ M/s.

**Ratio of Rate Constants $k_{23}/k_{24}$.** There are two methods to calculate the ratio $k_{23}/k_{24}$. One is based on eqs 7 and 8 under reaction conditions of Figure 1c; the other is based on eqs 9 and 10 under reaction conditions of Figure 1d. First, in the case of Figure 1c, the decreasing rate of 3 and increasing rate of 4 are equal (eq 8) after the first 10 min of reaction. If the decreasing IR peak of 3 is monitored, the observed rate constant $k_{obsd}$ can then be obtained by the use of eqs 11 and 12. This allows a

$$\ln [A_3(t)] = -k_{obsd}t + \text{constant} \qquad (11)$$

$$k_{obsd} = \frac{k_{32}k_{24}}{k_{23}[L] + k_{24}} \qquad (12)$$

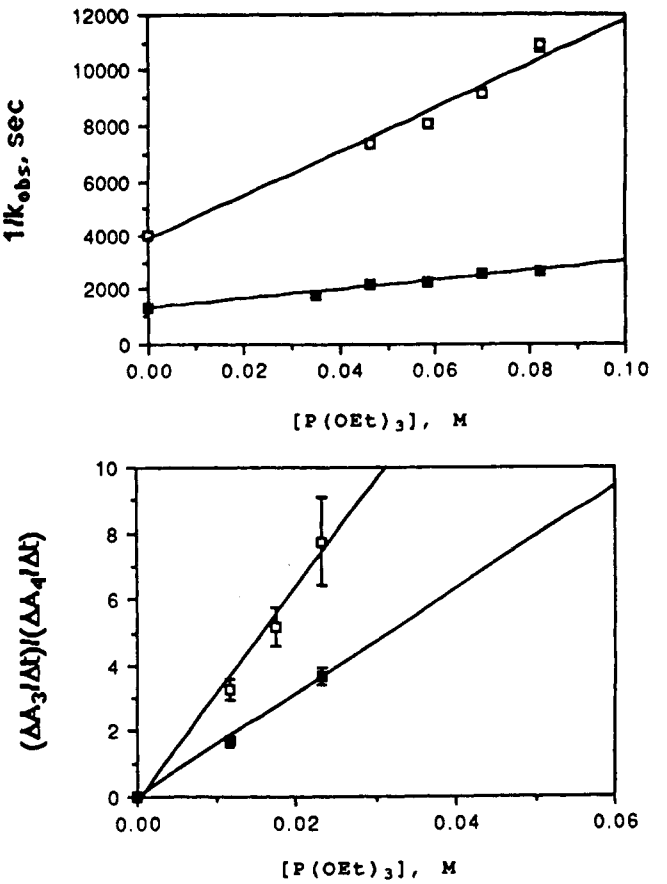


**Figure 3.** Evaluation of $k_{23}/k_{24}$ ratios: (a, top) plot of $1/k_{obsd}$ vs [P(OEt)$_3$] at high temperature for decreasing ($\eta^1$-Ind)Re(CO)$_3$[P(OEt)$_3$]$_2$ in decalin (eq 13), where □ = 100 °C and ■ = 90 °C; (b, bottom) plot of $(\Delta A_3/\Delta t)/\Delta A_4/\Delta t)$ vs [P(OEt)$_3$] at low temperature (eq 16), where □ = 70 °C and ■ = 50 °C.

calculation of the $k_{23}/k_{24}$ ratio from the observed rate constant of decreasing $\eta^1$-product (3). Rearranging eq 12 to its inverse form gives eq 13. A plot of $1/k_{obsd}$ vs [L]

$$\frac{1}{k_{obsd}} = \frac{1}{k_{32}}\frac{k_{23}}{k_{24}}[L] + \frac{1}{k_{32}} \qquad (13)$$

should be linear and have a nonzero intercept. Dividing the slope of this plot by its intercept gives the ratio of $k_{23}/k_{24}$, and the inverse of the intercept gives $k_{32}$. Experimental results show the plots are linear (Figure 3a), and the ratios of $k_{23}/k_{24}$ obtained from these plots are given in Table III. The $k_{32}$ value obtained using eq 12 ($k_{32}$ = 1.87 × $10^{-3}$ $s^{-1}$ at 100 °C) is in reasonable agreement with the value determined directly ($k_{32}$ = 7.67 × $10^{-4}$ $s^{-1}$) by starting with the isolated $\eta^1$-compound (3). Unfortunately, it was not possible to prepare the $\eta^1$-compound free of added ligand, so the rate is slower than that estimated from a steady-state treatment of the data due to retardation by the presence of free ligand.

The second method for estimating the ratio of $k_{23}/k_{24}$ makes use of data from the reaction condition of Figure 1d. Considering eq 9, the rate laws for each step are eqs 14 and 15. Dividing eq 14 by eq 15 causes the [A$_2$] term

$$\frac{d[A_3]}{dt} = k_{23}[L][A_2] \qquad (14)$$

$$\frac{d[A_4]}{dt} = k_{24}[A_2] \qquad (15)$$

to cancel and gives eq 16. A plot of $(d[A_3]/dt)/(d[A_4]/dt)$ vs [L] should be linear and go through the origin, and the slope of the line is the ratio of $k_{23}/k_{24}$. The left side of eq

$$\frac{\frac{d[A_3]}{dt}}{\frac{d[A_4]}{dt}} = \frac{k_{23}}{k_{24}}[L] \quad (16)$$

16 is readily obtained by applying the initial rate approximation (i.e., $d[A]/dt = \Delta[A]/\Delta t$). The origin (0, 0) is added to both of the cases ($T$ = 70 and 56 °C) to get more reasonable results (Figure 3b). The results of $k_{23}/k_{24}$ obtained from this plot are given in Table III. Since the ratios of $k_{23}/k_{24}$ in Table III were obtained by two different methods (eq 13 is used for those of 100 and 90 °C, while eq 16 is used for those of 70 and 56 °C), it is necessary to check the validity that the two methods do in fact deal with the same $k_{23}$ and $k_{24}$ albeit at different temperatures. One way to test this is to see if the enthalpy differences and entropy differences of the two steps (2 → 3 and 2 → 4) can be obtained from a plot of ln ($k_{23}/k_{24}$) vs $1/T$. Such a plot should be linear providing $k_{23}$ and $k_{24}$ are measuring the same pathway rates at all four temperatures. The good correlation coefficient ($R^2$ = 0.99) of this plot indicates that the $k_{23}/k_{24}$ ratios obtained from two different computational methods are a valid measure of the intended pathways 2 → 3 and 2 → 4 for $k_{23}$ and $k_{24}$, respectively.

With reference to eq 9, it appears that the entropy difference of the two steps, $\Delta S_{23}^{\ddagger} - \Delta S_{24}^{\ddagger}$, should have a large negative value, because $\Delta S_{23}^{\ddagger} < 0$ (adding more ligand) and $\Delta S_{24}^{\ddagger} > 0$ (losing one CO ligand). Furthermore, since the $\eta^5$-product forms more readily at high than at low temperatures, $\Delta H_{24}^{\ddagger}$ is expected to be larger than $\Delta H_{23}^{\ddagger}$ and give a negative value for the difference $\Delta H_{23}^{\ddagger} - \Delta H_{24}^{\ddagger}$. The anticipated negative entropy and enthalpy differences between pathways 2 → 3 and 2 → 4 are in accordance with experiment (Table III).

The ratio of rate constants $k_{23}/k_{24}$ provide interesting results. For example, the value of $k_{23}/k_{24}$ decrease (Table III) with increase in temperature. This means that the $\eta^1$-product (3) is less favored at higher temperature relative to lower temperature, which agrees with the experimental plots (Figure 1) of spectral changes during the reaction of 1 with $P(OEt)_3$. Based on the $k_{23}/k_{24}$ values in Table III, it is possible to estimate the initial amount of $\eta^1$-species formed relative to $\eta^5$-product. The relative amount of $\eta^1$- and $\eta^5$-products formed depend on the temperature and on the ligand concentration, being given by the ratio $k_{23}$-$[L]/k_{24}$ (see eq 16). At conditions of $T$ = 56 °C and [L] = 0.082 M, $k_{23}/k_{24}$ = 324 (Table III) and $k_{23}[L]/k_{24}$ = 26.57. Thus, there is 26 times more $\eta^1$- than $\eta^2$-product, which corresponds to 96% of $\eta^1$-product and 4% of $\eta^5$-product. Reaction at $T$ = 100 °C and [L] = 0.012 M allows similar estimates showing 32% is $\eta^1$-product while 68% is $\eta^5$-product. These results indicate how dependent the initial formation of $\eta^1$- and $\eta^5$-species is on the reaction temperature and/or ligand concentration.

**Simulated Curves and Experimental Results.** The rate law for each elementary step based on Scheme I can be expressed by eqs 17–20. By application of the steady-state condition for the $\eta^3$-intermediate of $d[A_2]/dt = 0$ and without consideration of the reaction conditions mentioned previously (Figure 1a–d), these differential equations (eqs 17–20) are readily solved using the Laplace transformation method.[9] In this treatment the concentration of each species is expressed as an exponential function of $k_{12}$, $k_{32}$, $k_{23}/k_{24}$, and of time (s). The solution of these differential equations is available as supplementary material. Since most of the values for the rate constants of each of the elementary steps are known, assumptions made for each case can be checked directly. Also this treatment is a test of the validity of these rate constants derived for the elementary steps at the different experimental conditions and for the proposed mechanism. On the basis of the solution of the differential equations (eqs 17–20), the simulated curves (the molar absorbancy of species 1, 3, and 4) can be simplified by using the rate constant values in Table III to give eqs 21–23 for the reaction at 100 °C, where $k_{12}$ = 0.105 $M^{-1}$ $s^{-1}$, $k_{23}/k_{24}$ = 40, $k_{32}$ = 1.8 × 10⁻13 $s^{-1}$, and [L] = 0.058. Here $Abs_i(t)$ is the molar absorbancy of species $i$. The resulting simulated curves from these equations can then be directly compared with the experimental results (see Figure 1c for above mentioned example). That the simulated plots estimated in this manner are in good agreement with the experimental points of the spectral changes (Figure 1a–d) is strong supporting evidence for the proposed mechanism. The results require that the $\eta^1$-3 and the $\eta^5$-species (4) be formed from the same intermediate.

$$\frac{d[A_1]}{dt} = k_{12}[L][A_1] \quad (17)$$

$$\frac{d[A_2]}{dt} = k_{12}[L][A_1] - (k_{23}[L] + k_{24})[A_2] + k_{32}[A_3] \quad (18)$$

$$\frac{d[A_3]}{dt} = k_{23}[L][A_2] - k_{32}[A_3] \quad (19)$$

$$\frac{d[A_4]}{dt} = k_{24}[A_2] \quad (20)$$

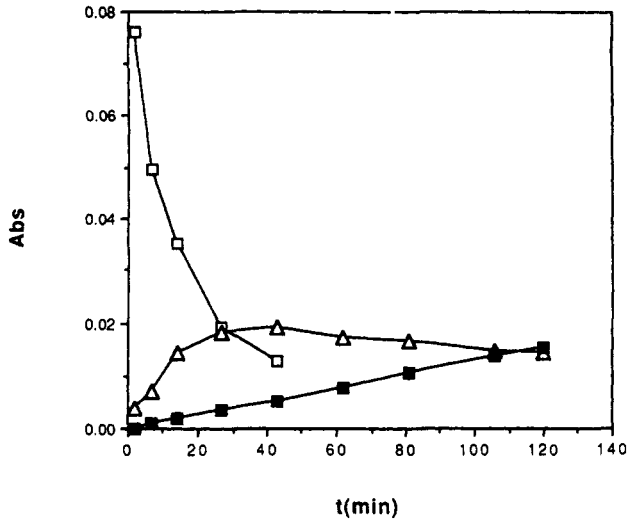


**Figure 4.** Absorption changes of each species for the reaction of $(\eta^5\text{-}TdH_2)Re(CO)_3$ with $P(OEt)_3$ (0.082 M) in decalin at 70 °C. The symbols are □ = $(\eta^5\text{-}TdH_2)Re(CO)_3$, △ = $(\eta^1\text{-}TdH_2)Re(CO)_3[P(OEt)_3]_2$, and ■ = $(\eta^5\text{-}TdH_2)Re(CO)_2P(OEt)_3$.

$$[Abs_1(t)] = [Abs_1(0)] \exp\{-0.0061t\} \quad (21)$$

$$[Abs_3(t)] = -0.77[Abs_1(t)](\exp\{-0.0061t\} - \exp\{-0.00054t\}) \quad (22)$$

$$[Abs_4(t)] = [Abs_1(0)](1 - 0.23 \exp\{-0.0057t\} - 0.77 \exp\{-0.00054t\}) \quad (23)$$

**Effect of Entering Nucleophile.** It has long been known in chemistry generally that the strength of a nucleophile depends on its electronic and its steric properties. In some cases such as for the CO substitution of $(\eta^5\text{-}C_5H_5)Rh(CO)_2$, electronic factors predominate and the rates of reaction qualitatively respond to the basicities of

(9) Steinfeld, J. I.; Francisco, J. S.; Hase, W. L. *Chemical Kinetics and Dynamics*; Prentice Hall: Englewood Cliffs, NJ, 1989.

the nucleophiles.[1b] However, for the analogous more sterically encumbered compounds $(\eta^5\text{-}C_5(CH_3)_5)Rh(CO)_2$, steric factors predominate and the rates of reaction qualitatively respond to the cone angles[10] of the nucleophiles.[11] Quantitative detailed studies[12] of these steric–electronic factors have been made in an attempt to separate the steric and the electronic factors that contribute to the strengths of nucleophiles.

No systematic study of nucleophilic strength was made in this study, but the reactivities of a very few phosphines and phosphites were examined. The free energies for the initial associative reactions of $(\eta^5\text{-Ind})Re(CO)_3$ via pathways $k_{12}$ (Scheme I) are given in Table V. It comes as no surprise that $P(CH_3)_3$, having a small cone angle and being a strong base, is the strongest nucleophile. Likewise of no surprise is the observation that the base $P(OPh)_3$ is a poor nucleophile.

A somewhat different point that needs to be made is that the different nucleophiles differ in their tendencies to form $\eta^1$-**3** versus $\eta^5$-**4** products. For example the reaction of **1** with $P(OPh)_3$ at 100 °C affords only the $\eta^5$-**4** product, whereas the reaction of **1** with $P(n\text{-Bu})_3$ forms only the $\eta^1$-product, which is stable at 60 °C for 1 h and decomposes rapidly at 90 °C. Furthermore, $P(OEt)_3$ reacts with **1** at different conditions to afford an $\eta^1$- or an $\eta^5$-product or a mixture of both. Note that these three nucleophiles have similar cone angles but greatly differ in basicity (Table V). This suggests that a preference for $\eta^1$- or $\eta^5$-products depends on electronic factors. We thank a reviewer for what appears to be a plausible explanation of this observation. Her/his explanation, as stated in the referee report, is "... the strongly basic phosphines increase the electron density on the metal and simultaneously enhance M–CO bonding which would slow the dissociation of the CO ligand and the formation of the $\eta^5$-product." However, steric factors may also contribute to the preference for $\eta^1$- or $\eta^5$-products. For example, the nucleophiles $PCy_3$, $P(n\text{-Bu})_3$, and $PMe_3$ with similar basicities but markedly different core angles (Table V) all afford $\eta^1$-products. Yet for $PCy_3$, with a very large cone angle, $\eta^1$ is a minor product and it is readily converted into the $\eta^5$-product. This indicates that in spite of its strong basicity, the large size of $PCy_3$ sterically promotes Re–CO bond rupture and favors formation of the $\eta^5$-product. Thus, steric factors are also important, and a much more detailed study is required to delineate the relative importance of steric and inductive effects of the nucleophiles in these reactions toward the formation of $\eta^1$- or $\eta^5$-products.

As a further test of the mechanism represented by Scheme I, it was decided to use the bidentate ligand diphos, $Ph_2PC_2H_4PPh_2$. This ligand is similar in basicity and cone angle to $PMePh_2$, but because of the strong chelating tendency of diphos it was believed that the chelate ring of $(\eta^1\text{-Ind})Re(CO)_3$(diphos) once formed would not reopen (**3** ↛ **2**, Scheme I) and thus no $\eta^5$-**4** product would form. This is in accord with what was observed experimentally, where only $\eta^1$-**3** was detected regardless of the reaction conditions. This differs from the earlier report[6] that the reaction of $(\eta^5\text{-Ind})Re(CO)_3$ with 2,2′-bipyridine does not give $(\eta^1\text{-Ind})Re(CO)_3$(bpy), which was prepared indirectly.

**Comparison with Trindenyl Analogues.** It is expected that the trindenyl systems (structures II–IV) will react by mechanisms similar to that of $(\eta^5\text{-Ind})Re(CO)_3$. The reaction of $(\eta^5\text{-TdH}_2)Re(CO)_3$ (structure II) with $P(OEt)_3$ at 40 °C showed spectral changes consistent with the $\eta^5$-**1′** → $\eta^3$-**2′** → $\eta^1$-**3′** conversion of the indenyl analogues (Scheme I). At 80 °C spectral changes correspond with the initial rapid formation of $\eta^1$-**3′** followed by its conversion to the $\eta^5$-**4′** product (Scheme II). The rates of disappearance of the $\eta^5$-**1′** trindenyl substrates of Re and of Rh with added nucleophile are second-order and are presumed to involve the pathways $\eta^5$-**1′** → $\eta^3$-**2′** (Scheme II).

**Scheme II**

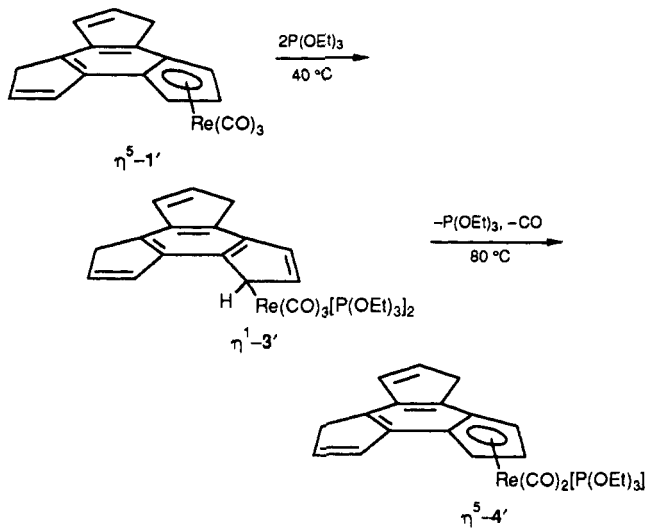


The free energies of activation, $\Delta G_{12}^{\ddagger}$, for the reactions of $(\eta^5\text{-Td})[Re(CO)_3]_3$ and $(\eta^5\text{-Td})[Rh(CO)_2]_3$ are given in Table VIII and compared with corresponding reactions of analogous cyclopentadienyl- and indenylmetal complexes. The reactivities decrease in the order Ind > Td > Cp, which is consistent with the ease of localizing a pair of electrons on the cyclic ligand in order to allow for nucleophilic attack of a low-energy metal orbital.[1b]

**The indenyl ligand effect** contributes less to the reactivity of the Td than of the Ind system. For Mn, only the indenyl complex $(\eta^5\text{-Ind})Mn(CO)_3$ reacts at the experimental conditions used. Also consistent with the driving force for reaction being the aromaticity of $\pi$-delocalization in the central six-membered ring is the observation that the rates of reaction decrease in the order II > III > IV, where $t_{1/2}$ equal 7 min, 11 min, and no reaction, respectively, for reactions of trindenyl complexes at room temperature with 0.06 M $PMe_2Ph$ solution of THF.

Finally, kinetic data in Table VIII show that, for a given $(\eta^5\text{-L})M(CO)_n$, the reactivities for metal changes decrease in the order Rh > Re > Mn. That Rh is the fastest to react seems reasonable because its lower coordination number of 5, rather than 6 for the Re and Mn compounds, would permit more ready expansion of its coordination number in order to better accommodate the associative reactions $\eta^5$-**1** → $\eta^3$-**2**. It may appear strange to find Re reacting much faster than does Mn, because it is well-known that CO substitution of $Mn(CO)_5X$[13] is faster than that of $Re(CO)_5X$.[14] However, these CO substitution reactions are dissociative, which means a M–CO bond-breaking process with an accompanying decrease in coordination

(10) Tolman, C. A. *Chem. Rev.* **1977**, *77*, 313.
(11) Rerek, M. E., Ph.D. Thesis, Northwestern University, Evanston, IL, 1984; pp 46, 47.
(12) (a) Poë, A. J. *Pure Appl. Chem.* **1988**, *60*, 1209. (b) Liu, H. Y.; Eriks, K.; Prock, A.; Giering, W. P. *Organometallics* **1990**, *9*, 1758.
(13) Angelici, R. J.; Basolo, F. *J. Am. Chem. Soc.* **1962**, *84*, 2495.
(14) (a) Zingales, F.; Graziani, M.; Faraone, F.; Belluco, U. *Inorg. Chim. Acta* **1967**, *1* (1), 172. (b) Howell, J. A. S.; Burkinshaw, P. M. *Chem. Rev.* **1983**, *83*, 56.

number. Instead the associative pathway of $k_{12}[L]$ (Scheme I) requires an increase in coordination number, which is presumably more readily achieved due to the large size of Re relative to the smaller Mn.[15]

**Conclusion.** Rather extensive kinetic studies were made of the reaction of ($\eta^5$-Ind)Re(CO)$_3$ with P(OEt)$_3$, and it was observed that at four different experimental conditions of temperature and P(OEt)$_3$ concentration the reaction progress and its products differ. Low temperatures and high concentrations of P(OEt)$_3$ favor the formation of $\eta^1$-**3**, whereas high temperatures and low concentrations of P(OEt)$_3$ favor the formation of $\eta^5$-**4**. The treatment of experimental data at four different reaction conditions allows for good agreement between experimental and simulated absorbancy changes during reaction, providing the $\eta^1$-**3** and $\eta^5$-**4** products come from the same active intermediate (Scheme I). The exact nature of this intermediate is not known, but on the basis of known ring-slippage[2] organometallic chemistry, it appears the intermediate should be $\eta^3$-**2**.

The nature of the entering nucleophile also plays a major role in the distribution of products $\eta^1$-**3** versus $\eta^5$-**4**. In general a nucleophile that is a strong base and has a small cone angle (P(CH$_3$)$_3$) favors formation of $\eta^1$-**3**, whereas one that is a weak base with a larger cone angle (P(OPh)$_3$) favors the $\eta^5$-**4** products. The kinetic indenyl ligand effect is observed to a lesser extent with trindenylmetal complexes, and in general the rates of reaction for analogous metal compounds decrease in the order Ind > Td > Cp. This is in accord with a decrease in $\pi$-delocalization of the electron density in the transition state/active intermediate for reaction. Finally, for the same system but different metal the rates of reaction decrease in the order Rh > Re > Mn. This order seems reasonable for these associative reactions with attack on the metal, because Rh is only 5-coordinate and because Re is larger than Mn.

**Acknowledgment.** We wish to thank Dr. Jeffrey W. Freeman for doing some of the preliminary kinetic experiments, Dr. Merritt C. Helvenston for preparing some of the compounds, and one of the reviewers for explaining the inductive contribution to the nucleophile specificity in the formation of $\eta^1$- or $\eta^5$-products. We also thank the National Science Foundation for its support of this research and Johnson-Matthey for the generous loan of rhodium salts.

**Registry No.** **1**, 33308-86-0; **3**, 137365-88-9; **4**, 137365-92-5; ($\eta^1$-Ind)Re(CO)$_3$[P($n$-Bu)$_3$]$_2$, 93757-34-7; ($\eta^1$-Ind)Re(CO)$_3$[P(OPh)$_3$]$_2$, 137365-89-0; ($\eta^1$-Ind)Re(CO)$_3$(diphos), 137365-90-3; ($\eta^1$-Ind)Re(CO)$_3$[PCy$_3$]$_2$, 137365-91-4; ($\eta^5$-Ind)Re(CO)$_2$[P(OPh)$_3$], 137365-93-6; ($\eta^5$-Ind)Re(CO)$_2$[PCy$_3$], 137365-94-7; ($\eta^5$-TdH$_2$)Re(CO)$_3$, 121619-84-9; ($\eta^1$-TdH$_2$)Re(CO)$_3$[P(OEt)$_3$]$_2$, 137365-95-8; ($\eta^1$-TdH$_2$)Re(CO)$_2$[P(OEt)$_3$], 137365-96-9; ($\eta^5$-Td)[Re(CO)$_3$]$_3$, 121653-41-6; ($\eta^1$-Td)[Re(CO)$_3$[P($n$-Bu)$_3$]$_2$]$_3$, 137393-40-9; ($\eta^5$-Td)[Re(CO)$_2$P($n$-Bu)$_3$]$_3$, 137365-97-0; ($\eta^5$-Td)[Mn(CO)$_3$]$_3$, 121653-39-2; ($\eta^5$-Td)[Rh(CO)$_2$]$_3$, 137365-87-8; ($\eta^5$-Td)[Rh(CO)PPh$_3$]$_3$, 137365-98-1; ($\eta^5$-Td)[Rh(CO)P($n$-Bu)$_3$]$_3$, 137365-99-2; [Rh(COD)Cl]$_2$, 12092-47-6; ($\eta^5$-Td)[Rh(COD)]$_3$, 137365-86-7; TdH$_3$, 73255-13-7; PCy$_3$, 2622-14-2; P(OPh)$_3$, 2622-14-2; P(OEt)$_3$, 122-52-1; PMePh$_2$, 1486-28-8; diphos, 1663-45-2; P($n$-Bu)$_3$, 998-40-3; PMe$_2$Ph, 672-66-2; PMe$_3$, 594-09-2; ($\eta^5$-Cp)Rh(CO)$_2$, 12192-97-1; ($\eta^5$-Ind)Rh(CO)$_2$, 12153-10-5.

**Supplementary Material Available:** Derivations of the equations used to generate estimated simulated curves of spectral changes for reactions at the four different experimental conditions shown in Figure 1a–d (4 pages). Ordering information is given on any current masthead page.

(15) Walker, H. W.; Rattinger, G. B.; Belford, R. L.; Brown, T. L. *Organometallics* **1983**, *2*, 775.

# Synthesis and Electronic Structure of Permethylindenyl Complexes of Iron and Cobalt

Dermot O'Hare,*[†] Jennifer C. Green,*[†] Todd Marder,*[‡] Scott Collins,[‡] Graham Stringer,[‡] Ashok K. Kakkar,[‡] Nikolas Kaltsoyannis,[†] Alexander Kuhn,[†] Rhian Lewis,[†] Christian Mehnert,[†] Peter Scott,[†] Mohamedally Kurmoo,[†] and Stuart Pugh[†]

*Inorganic Chemistry Laboratory, South Parks Road, Oxford OX1 3QR, U.K., and Department of Chemistry, University of Waterloo, Waterloo, Ontario N2L 3G1, Canada*

*Received May 7, 1991*

Fe($\eta^5$-C$_9$Me$_7$)$_2$ and Co($\eta^5$-C$_9$Me$_7$)$_2$ have been prepared by treatment of either FeCl$_2$·$x$THF ($x \cong 2$) or Co(acac)$_2$ with LiInd* (Ind* = $\eta^5$-C$_9$Me$_7$) in THF. The cyclic voltammograms of both Fe($\eta^5$-C$_9$Me$_7$)$_2$ and Co($\eta^5$-C$_9$Me$_7$)$_2$ indicate that they are redox active with one-electron oxidations at $E_{1/2}$ = −0.32 and −1.05 V vs SCE, respectively; both complexes exhibit second oxidations at $E_{1/2}$ = 1.28 and 1.21 V vs SCE, respectively. The 17-electron and 18-electron cations [Fe($\eta^5$-C$_9$Me$_7$)$_2$]$^+$PF$_6^-$ and [Co($\eta^5$-C$_9$Me$_7$)$_2$]$^+$PF$_6^-$ were isolated by treatment of the neutral complexes with either [Fe($\eta^5$-C$_5$H$_5$)$_2$]$^+$PF$_6^-$ (for Fe) or NH$_4$PF$_6$ (for Co). Gas-phase UV photoelectron spectroscopy experiments on both Fe($\eta^5$-C$_9$Me$_7$)$_2$ and Co($\eta^5$-C$_9$Me$_7$)$_2$ show that the permethylindenyl ligand gives rise to lower first ionization energy (correlating with a more negative $E_{1/2}$ value) than the Cp* (Cp* = $\eta^5$-C$_5$Me$_5$) ligand for Fe, while in the Co analogue the reverse is found. EPR and magnetic susceptibility experiments on [Fe($\eta^5$-C$_9$Me$_7$)$_2$]$^+$PF$_6^-$ and Co($\eta^5$-C$_9$Me$_7$)$_2$ both in solution and the solid state yield magnetic moments of 2.09 $\mu_B$ for [Fe($\eta^5$-C$_9$Me$_7$)$_2$]$^+$PF$_6^-$ and 1.59 $\mu_B$ for Co($\eta^5$-C$_9$Me$_7$)$_2$.

## Introduction

Transition-metal indenyl compounds have attracted interest in recent years as an alternative to the cyclopentadienyl ligand for two main reasons. The relative ease of slippage of the indenyl ring from $\eta^5$ to $\eta^3$ coordination has been proposed to account for the enhanced reactivity in both $S_N1$[1-3] and $S_N2$[1-6] substitution reactions compared

[†] Inorganic Chemistry Laboratory.
[‡] University of Waterloo.

(1) O'Connor, J. M.; Casey, C. P. *Chem. Rev.* **1987**, *87*, 307.

0276-7333/92/2311-0048$03.00/0 